Charging of Dust Grains in Plasma with Energetic Electrons

Bob Walch
Department of Physics, University of Northern Colorado, Greeley, Colorado 80639

Mihály Horányi
Laboratory for Atmospheric and Space Physics, University of Colorado, Boulder, Colorado 80309-0392

Scott Robertson
Department of Astrophysical, Planetary, and Atmospheric Sciences, University of Colorado, Boulder, Colorado 80309-0391
(Received 13 March 1995)

The charge on small grains of glass, copper, graphite, and silicon has been measured in a plasma device containing both thermal electrons with energies of a few eV and monoenergetic suprathermal electrons. For conditions in which the charging current is dominated by suprathermal electrons, the grains charge to the potential that repels these electrons unless they induce significant secondary emission. The charge on the grains is linear with size for diameters from 30 to 120 μm and is the value expected from the grain capacitance and the charging potential.

PACS numbers: 52.25.Vy

Plasmas in the laboratory and in space [1–4] are frequently contaminated with small, charged dust particles. For example, dust is found in the interstellar medium [5], in the cometary environment, in planetary magnetospheres [6], in the upper atmosphere [7], and in industrial plasmas [8,9]. In these environments, particle dynamics is determined by gravity, molecular and plasma drag, radiation pressure, and electric and magnetic forces. The currents that contribute to charging include those due to incident electrons and ions, secondary electrons induced by electron and ion impact, and photoemission [10]. Thermionic emission and field emission can usually be ignored. Secondary emission is particularly important for dust in space [11,12] because the oxides and silicates in space dusts [13] have relatively high secondary emission coefficients. Models for the charging of dust grains have used theories for the current collected by Langmuir probes in the limit where collisions are unimportant and the size of the probe is small compared with the Debye length. There have been only a few experimental efforts to determine the charge on dust grains in plasmas [14–17]. We report the first systematic study of grain charging as a function of size, material properties, and electron energy.

For a grain in a Maxwellian plasma, the incident current, I_t, of thermal electrons and ions is given by

$$I_t/A = \begin{cases} J_i[1 - e\Phi/T_i] - J_e \exp[e\Phi/T_e], & e\Phi < 0, \\ J_i \exp[-e\Phi/T_i] - J_e[1 + e\Phi/T_e], & e\Phi > 0, \end{cases} \quad (1)$$

where A is the surface area of the grain, e is the magnitude of the charge on an electron, $J_i = ne(T_i/2\pi m_i)^{1/2}$ and $J_e = ne(T_e/2\pi m_e)^{1/2}$ are current densities, Φ is the grain potential relative to the plasma potential, T is the temperature in energy units, n is the density of electrons or singly charged ions, m is the particle mass, and the subscripts e and i refer to electrons and ions, respectively. In addition to thermal argon plasma, the experimental apparatus contains fast, nearly monoenergetic electrons with energy U. The net charging current, I_f, due to these electrons and the secondaries they create is

$$\begin{aligned} I_f/A &= -J_f[1 + e\Phi/U][1 - \delta], \\ &\approx -J_f[1 + e\Phi/U][1 - (U + e\Phi)/E_i], \\ &\quad -U < e\Phi, \end{aligned} \quad (2)$$

where J_f is the fast electron current to a surface at zero potential, the first bracketed term is from orbit-limited probe theory [18], and δ is the energy-dependent secondary emission coefficient. For simplicity, we assume that this coefficient varies linearly below the electron energy E_1 at which the coefficient is unity. The coefficient can then be written $\delta \approx (U + e\Phi)/E_1$, where $U + e\Phi$ is the energy at which the fast electrons strike the collecting surface. The temperatures of the thermal species are sufficiently low that they induce no secondary emission and photoemission is negligible. A similar model has been used to describe the current to Langmuir probes in plasmas with energetic electrons [19]. The grains charge to the floating potential, Φ_f, defined by $I_t + I_f = 0$. This potential is usually negative due to the greater mobility of electrons. The charge on the grains is determined by $Q = C\Phi_f$, where C is the capacitance of the grain. For an isolated sphere of radius r, $C = 4\pi\varepsilon_0 r$ and the charge is approximately 700 electrons per volt for a grain of 1 μm radius.

The experiment is performed by dropping individual dust grains through a plasma and having them fall into a

 0031-9007/95/75(5)/838(4)$06.00

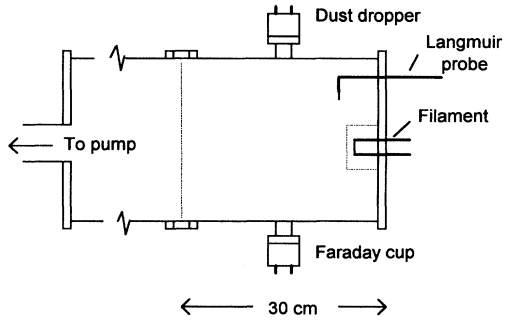

FIG. 1. Schematic diagram of the experimental apparatus. The dust is dropped into the plasma at the top of the device and falls into a Faraday cup in a diagnostic arm below the vacuum chamber.

Faraday cup below the plasma (Fig. 1). The Faraday cup is connected to a sensitive amplified, and the height of an output pulse indicates the grain charge [16]. The plasma is generated in one side of a double plasma (DP) machine [20], which has previously been described [16,21]. The 30 cm diameter $\times$ 30 cm long aluminum chamber has a heated filament at one end that may be biased from -15 to -120 V to inject 2 mA of fast electrons into the chamber. The base pressure is 4×10^{-7} Torr and the fill pressure is 2×10^{-6} Torr of argon. The fill pressure is much lower than ordinarily used in the DP machine in order to have the current of fast electrons, J_f, comparable to the electron saturation current, J_e. This condition increases secondary emission to the point where it is observable in the charging data. At higher fill pressure, the charging is primarily by the thermal electrons, and the effects of fast electrons and secondaries are not seen. In this case, the charge on grains may be altered in the sheath at the wall by changes in the current densities of thermal particles. At the low density used here, the charging is everywhere dominated by the fast electrons whose current density changes little in the sheath due to their high energy relative to the thermal energy.

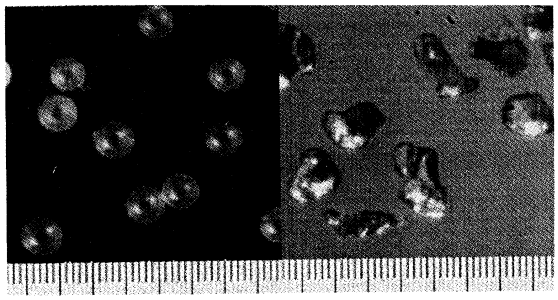

FIG. 2. Photomicrographs of the sieved dusts used in the experiments: glass microballoons (left) and graphite grains (right). The small scale divisions measure 10 μm. The grains have fallen through a mesh with 63 μm openings and were collected on a mesh with 53 μm openings. The grains of silicon and copper are similar in appearance to the graphite grains.

The dust dropper is a thin plate with a central hole through which the particles drop when the plate is moved by a pulse to an electromagnet. The pulse amplitude is adjusted so that the detected signals are primarily due to individual particles. Signals from multiple particles can be distinguished by their wave form and are not used. The dust grains used here (see Fig. 2) are (1) glass microballoons, selected for being spherical and to represent a substance with a high secondary emission coefficient; (2) graphite, selected for its low secondary emission coefficient; (3) copper, selected to represent a metallic conductor; and (4) silicon, selected because of its importance in plasma processing. The grains are sorted by size using screen mesh sieves, and the selected sizes range from 35 $\pm$ 5 to 115 $\pm$ 10 μm. The lower limit is set by the need to have a good signal-to-noise ratio in the charge measurements.

The current to a surface in the plasma is measured independently by a Langmuir probe. The probe tip is

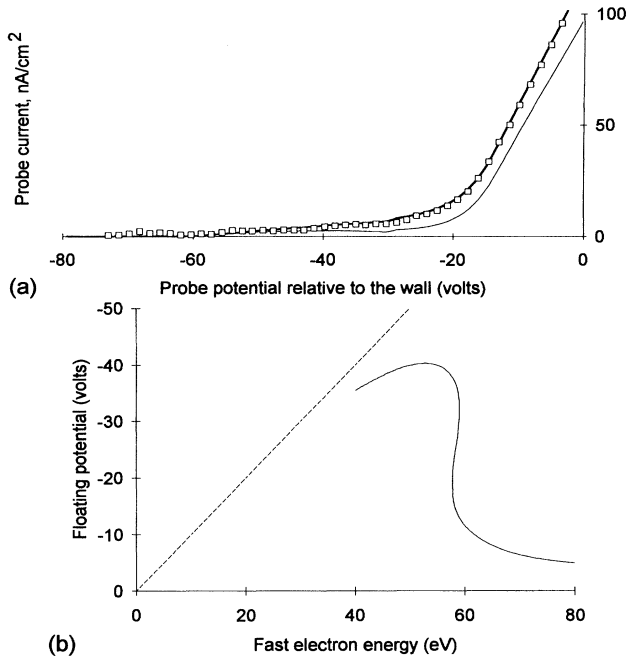

FIG. 3. (a) Plot of the current collected by the Langmuir probe as a function of bias voltage. The collection of electrons is defined as a positive current. The filament potential is -60 V. The squares are the data points, and the line between them is the fitted model. The lower line is the calculated current to a surface with the secondary emission characteristics of glass. (b) Plot of the floating potentials obtained from the model as a function of the fast electron energy. The floating potential with the smallest absolute value should be the observed potential when the grains begin their charging from zero potential. The assumed secondary emission coefficient is that of glass and the assumed plasma conditions are those in the experiment.

an 18 mm tungsten disk and orbit-limited probe theory applies to both the probe and the dust grains. Figure 3(a) shows probe data with a filament bias of −60 V. At probe potentials more negative than −60 V, fast and thermal electrons are repelled and only ion current is collected. As the probe is made less negative, the ion current decreases and fast electrons are collected. At potentials less negative than about −25 V thermal electrons are collected. The plasma potential, the point where the probe characteristic changes from exponential to linear, is −14 V with respect to the vacuum chamber at the position of the probe (a few cm from the wall). The fitted model for the total current, $I_t + I_f$ [given by Eqs. (1) and (2)], yields $J_f = 15$ nA/cm^2, $J_e = 27$ nA/cm^2, $T_e = 4.8$ eV, and J_i is too small to be accurately determined. The incident electron energy at which the secondary emission would exceed unity (E_1) is set in the model to the tabulated value for tungsten of 250 eV [22]. The charging time for a particle of diameter 50 μm to a potential of −30 V in a current of density of 30 nA/cm^2 is approximately 30 ms which corresponds to 6 cm of flight at the exit velocity of 2 m/s.

The current collected by a probe surface with the secondary emission characteristics of the glass spheres can be found from the model by changing the value of E_1 from that of tungsten to the value for glass (40 eV). This curve, shown by the lower solid line in Fig. 3(a), has a shallow minimum near −30 V. There are three possible floating potentials when this minimum lies below the axis. For example, in Fig. 33(b) the calculated floating potentials for glass as a function of fast electron energy are plotted for the conditions in the experiment and with the assumption $T_e/T_i = 10$. There are three floating potentials for fast electron energies from 57 to 59 eV. The grains enter the plasma at zero potential, initially collect a surplus of electrons, and the grain potential falls until the first zero crossing is encountered. For conditions where there are three floating potentials, the center floating potential is unstable because a small deviation from this potential results in charging to the neighboring stable potential. For conditions where there is a minimum just touching the axis, small fluctuations in plasma conditions may give grains access to both the first and third floating potentials.

The measured charge on angular graphite grains and on hollow glass microspheres with size in the range 53–63 μm is shown in Fig. 4. Also shown is the charge expected from the capacitance calculated for spheres of the median diameter with the assumption that the grains charge to the potential on the filament emitting the fast electrons. At fast electron energies below 25 eV, there is little ionization of the background gas, and it is expected that the grains will charge to the filament potential as observed. For graphite grains, the potential follows the potential on the emissive filament for potentials from −15 to −90 V. At more negative filament potentials the

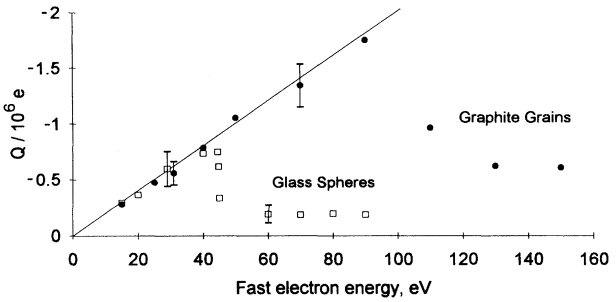

FIG. 4. Charge on glass spheres (open squares) and graphite grains (filled circles) as a function of the fast electron energy determined from the difference between the filament potential and the floating potential. The latter goes to zero at the wall. In Figs. 4, 5, and 6, the charge is in units of the electron charge, each point is an average of 50 measurements, and the error bars are 1 standard deviation above and below the mean. The solid line is the charge expected if the grains charge to the filament potential.

charge on graphite begins to decrease in magnitude due to secondary emission and the collection of ions created by the higher energy electrons. For glass microspheres, the charge decreases abruptly at an electron energy of 44.5 eV, which is slightly above the energy of 40 eV at which the secondary emission exceeds unity [22]. An abrupt decrease is expected when the plot of current as a function of potential has a minimum, which has been lowered to the point of touching the axis [Fig. 3(a), lower curve] through varying the fast electron energy. The new floating potential is the point where the thermal electrons collected from the tail of the Maxwellian are sufficient to offset the other currents. This balance occurs at a potential of a few times $-T_e/e$ as a result of the exponential dependence of the assumed Maxwellian distribution. Figure 5 shows both the measured and calculated charges on glass spheres of other sizes at a fixed fast electron of 40 eV. The charge scales linearly with the diameter and, below the energy threshold

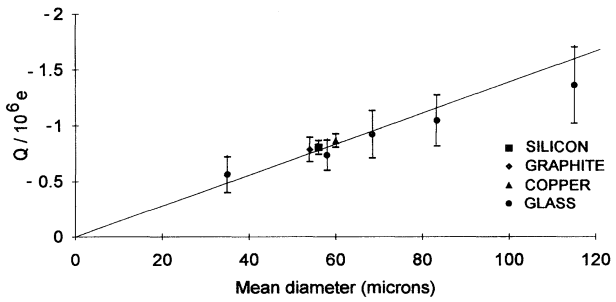

FIG. 5. Charge as a function of mean diameter. The glass samples used have sizes in the range 30–40, 53–63, 63–74, 74–95, and 105–125 μm. The data for silicon, graphite, and copper at 53–63 μm have been displayed horizontally for clarity. The line is the charge expected if the grains charge to the filament potential of −40 V.

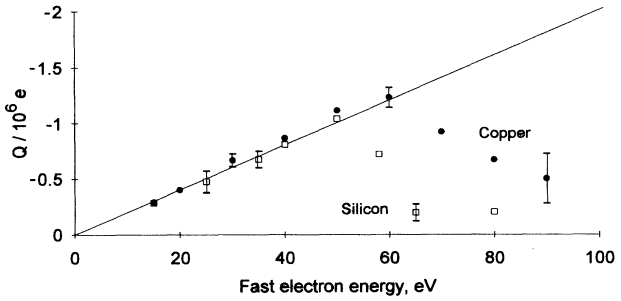

FIG. 6. Data for the charging of silicon grains (open squares) and copper grains (filled circles).

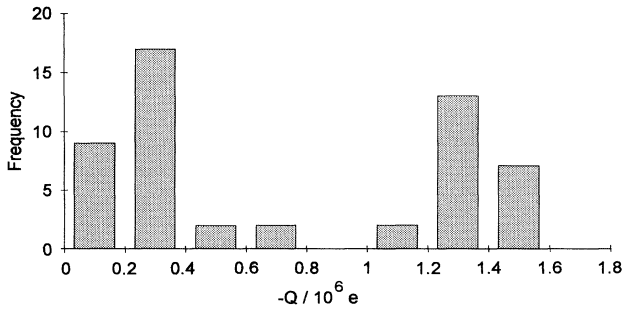

FIG. 7. Histogram of the measured charge on each of 50 silicon grains with diameters of 53–63 μm when the fast electron energy is set to the transition energy of 58 eV. The charge is approximately 20 000 electrons/V; thus the two peaks correspond to charging potentials of approximately −15 and −60 V.

for reduced charging, is the value expected from the calculated capacitance and filament potential. These grains are all much smaller than the Debye length which is a few cm.

Data for grains of silicon and copper are shown in Fig. 6. The charge on silicon grains behaves similarly to that on glass showing a transition to lower charge at an incident electron energy of 58 eV. The tabulated value of E_1 for silicon (120 eV) indicates that this transition should occur at higher energy than 58 eV. The observed behavior is likely to be due to the presence of an oxide coating resulting in secondary emission more like that of glass which contains silicon dioxide. The data for copper (E_1 = 200 eV) are similar to that of graphite (E_1 = 250 eV), which is consistent with the similarity in their secondary emission.

The distribution in the charge on silicon and glass grains is bimodal at the electron energy where the charging abruptly decreases. This is most clearly seen in the data for silicon at a fast electron energy of 58 eV (see Fig. 7), which shows that some grains charge to a potential near −58 V and that other grains charge to a potential near −15 V. The lack of a unique value may be due to fluctuations in the plasma parameters or small differences in the particles. The simultaneous appearance of more than one floating potential is interesting because it has been argued that, if one of the two floating potentials is positive, the electrostatic force will increase the rate of aggregation of small particles into larger particles [23].

The authors acknowledge support from the National Aeronautics and Space Administration (NASA) and the NASA Join Venture Program.

[1] C. K. Goertz, Rev. Geophys. **27**, 271 (1989).
[2] U. de Angelis, Phys. Scr. **45**, 465 (1992).
[3] T. G. Northrop, Phys. Scr. **45**, 475 (1992).
[4] D. A. Mendis and M. Rosenberg, Annu. Rev. Astron. Astrophys. **32**, 419 (1994).
[5] L. Spitzer, Jr., *Physical Processes in the Interstellar Medium* (Wiley, New York, 1982).
[6] E. Grün, G. E. Morfill, and D. A. Mendis, in *Planetary Rings,* edited by R. Greenberg and A. Brahic (University of Arizona Press, Tucson, 1984), p. 275.
[7] D. M. Hunten, R. P. Turco, and O. B. Toon, J. Atmos. Sci. **37**, 1342 (1980).
[8] G. S. Selwyn, J. Singh, and R. S. Bennett, J. Vac. Sci. Technol. A **7**, 2758 (1989).
[9] R. M. Roth, K. G. Spears, G. D. Stein, and G. Wong, Appl. Phys. Lett. **46**, 253 (1985).
[10] E. C. Whipple, Rep. Prog. Phys. **44**, 1197 (1981).
[11] V. W. Chow, D. A. Mendis, and M. Rosenberg, J. Geophys. Res. **98**, 19 065 (1993).
[12] V. W. Chow, D. A. Mendis, and M. Rosenberg, IEEE Trans. Plasma Sci. **22**, 179 (1994).
[13] E. E. Salpeter, Annu. Rev. Astron. Astrophys. **15**, 267 (1977).
[14] A. Barkan, N. D'Angelo, and R. L. Merlino, Phys. Rev. Lett. **73**, 3093 (1994).
[15] R. C. Hazelton and E. J. Yadlowsky, IEEE Trans. Plasma Sci. **22**, 91 (1994).
[16] B. Walch, M. Horányi, and S. Robertson, IEEE Trans. Plasma Sci. **22**, 97 (1994).
[17] A. Melzer, T. Trottenberg, and A. Piel, Phys. Lett. A **191**, 301 (1994).
[18] N. Hershkowitz, in *Plasma Diagnostics,* edited by O. Auciello and D. Flamm (Academic Press, San Diego, 1989), p. 113.
[19] C.-H. Nam, N. Hershkowitz, M. H. Cho, T. Intrator, and D. Diebold, J. Appl. Phys. **63**, 5674 (1988).
[20] R. J. Taylor, K. R. Mackenzie, and H. Ikezi, Rev. Sci. Instrum. **43**, 1675 (1972).
[21] H. Ikezi, R. P. H. Chang, and R. Stern, Phys. Rev. Lett. **36**, 1047 (1976).
[22] D. J. Gibbons, in *Handbook of Vacuum Physics,* edited by A. H. Beck (Pergamon, Oxford, 1966),Vol. 2, p. 301.
[23] M. Horányi and C. K. Goertz, Astrophys. J. **361**, 155 (1990).

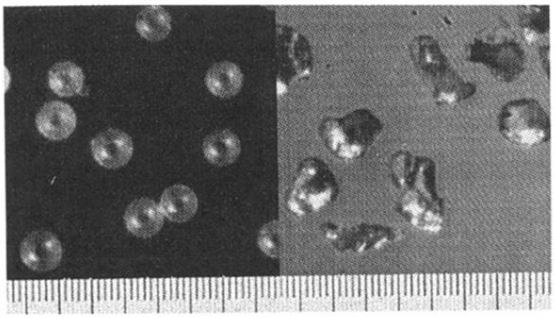

FIG. 2. Photomicrographs of the sieved dusts used in the experiments: glass microballoons (left) and graphite grains (right). The small scale divisions measure 10 μm. The grains have fallen through a mesh with 63 μm openings and were collected on a mesh with 53 μm openings. The grains of silicon and copper are similar in appearance to the graphite grains.